A comparison between molecular dynamics and X-ray results for dissociated CO in myoglobin

Dennis Vitkup[1,2,4], Gregory A. Petsko[1,3] and Martin Karplus[4,5]

The distribution of carbon monoxide after photodissociation in the myoglobin haem pocket has been investigated using molecular dynamics simulations at 300 K. The results show that both intermediates (one close to the haem iron and one further away) observed in recent low temperature X-ray studies of photodissociated CO have a high probability of occurrence, even at ambient temperatures. The fact that the O of CO is oriented toward the haem iron in the closer intermediate provides an explanation for the slow rate of CO geminate rebinding. A refinement against X-ray data generated from the molecular dynamics simulations indicates that the CO has a broader distribution in the haem pocket than is apparent from the experimental electron density. This effect is likely to be general for systems containing highly mobile groups.

The dynamics of ligand binding to myoglobin and haemoglobin is a fundamental problem in structural biology[1]. The ability of these proteins to discriminate between binding of O_2 and CO is of great biological importance[2]; while a CO molecule binds about 1000 times more strongly to a free haem than the natural ligand O_2, the protein is able to reduce that ratio to about 30:1[2,3]. Such high selectivity enables myoglobin and haemoglobin to serve as oxygen carriers without being inactivated by CO. Apart from its biological importance, the behaviour of both the ligand and the protein is of interest as a paradigm of protein dynamics. Experimental and theoretical studies have demonstrated the inherent complexity of this apparently simple ligand binding reaction[4,5]. A number of simulations of photodissociated ligands primarily concerned with ligand relaxation[6], or with ligand recombination and escape from the haem pocket[7–9], have been published.

In spite of considerable attention given to the reaction, the initial stages of the ligand motion after photodissociation are still not well understood. New information about the early events after photodissociation has been provided by recent low temperature X-ray structures reported by Schlichting *et al.*[10], Teng *et al.*[11] and Hartmann *et al.*[12], as well as by the femtosecond infra-red measurements of Lim *et al.*[13,14]. Two different positions for the photodissociated CO in the haem pocket were observed by Schlichting *et al.*[10] and by Teng *et al.*[11] Hartmann *et al.*[12] observed both CO positions.

The present paper describes results of molecular dynamics simulations of photodissociated myoglobin at room temperature that aid in the interpretation of the X-ray results. Multiple dissociation trajectories of a CO molecule in myoglobin were used to obtain positional and angular distributions for the CO in the haem pocket. Although the distributions are rather broad, there are two high probability sites for unbound CO in the pocket that correspond approximately with the X-ray results.

Electron densities calculated from the simulations suggest that the X-ray results for the CO positions after photodissociation are more confined than the CO is in reality. This type of effect is expected also for short time (nanosecond) X-ray measurements on mobile systems. The present study demonstrates the importance of molecular dynamics simulations as a complement to experimental measurements of time-dependent events in complex biological systems (detailed descriptions of the simulation methodology and the results will be published elsewhere).

CO distribution in the haem pocket after dissociation

Twenty-eight independent trajectories were calculated at 300 K for photodissociated CO in myoglobin with a solvent shell of 492 water molecules. Each dissociation reaction was started at a different point on an equilibrated MbCO trajectory and continued for 10 ps after dissociation. Data from all trajectories were combined to construct the probability distribution for the CO molecule in the haem pocket. There is considerable heterogeneity among the trajectories, but the present report focuses on the average results.

An analysis of the time dependence of the CO distribution function shows that it becomes independent of time in less than

[1]Rosenstiel Basic Medical Sciences Research Center, Brandeis University, Waltham, Massachusetts 02254, USA,
[2]Department of Biology, Program in Biophysics,Brandeis University, Waltham, Massachusetts 02254, USA,
[3]Departments of Chemistry and Biochemistry, Brandeis University, Waltham, Massachusetts 02254, USA,
[4]Department of Chemistry and Chemical Biology, Harvard University Cambridge, Massachusetts 02138, USA, [5]Laboratoire de Chimie Biophysique, Institut le Bel, Université Louis Pasteur 67000 Strasbourg, France

Correspondence should be addressed to M.K. *marci@tammy.harvard.edu*

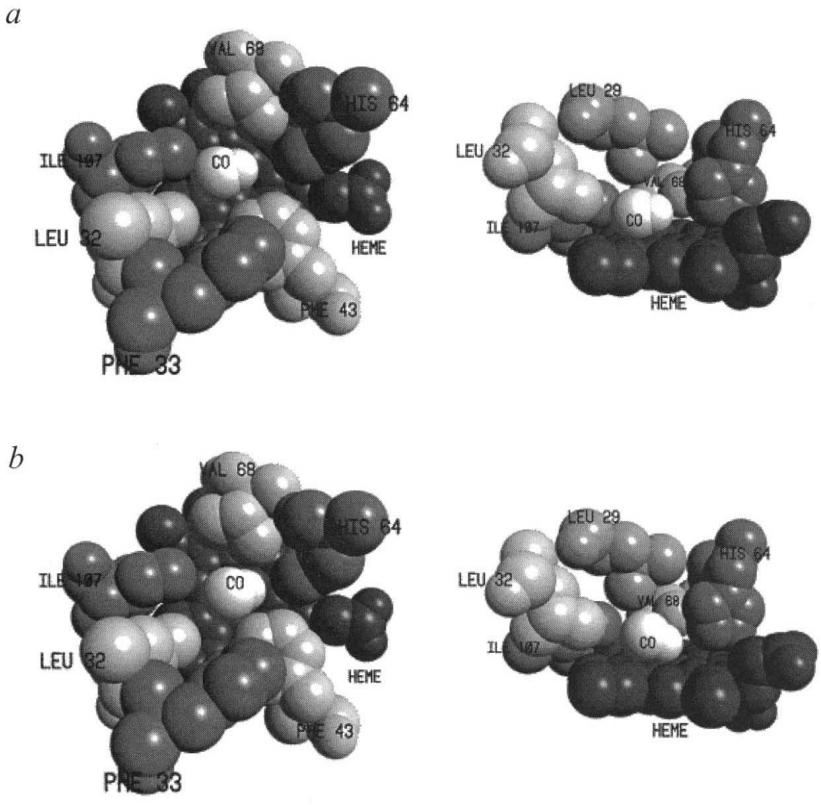

Fig. 1 Space-filling model of haem pocket with unbound CO molecule based on two low temperature X-ray studies by Schlichting *et al.*[10] and Teng *et al.*[11]. *a*, Structure obtained by at Schlichting *et al.*[10] at 20 K. *b*, Structure obtained by Teng *et al.*[11] at 40 K. Different grey scales are used for different pocket forming residues and the haem. The same orientation of the pocket is used in (*a*) and (*b*). On the left hand side of both panels the view is from distal side of the pocket down to the haem; the haem group is in the plane of the figure. All residues forming the haem pocket are shown except Leu 29 because it would obscure the CO molecule. On the right hand side of the panels the view from the side of the pocket is shown; two residues, Phe 43 and Phe 33, are not shown. The CO molecule is shown on both pictures with it oxygen atom closer to the iron.

1 ps (D.V., G.A.P. and M.K., unpublished results). This is in agreement with the results of femtosecond infra-red measurements[13,14], which indicate that unbound metastable states are formed within 300–500 fs after dissociation. Since the spectrum of unbound CO in the pocket does not change for hundreds of nanoseconds[13], the CO distribution appears to remain unchanged for a time much longer than the simulations.

The ligand is found to be constrained in its motion to a thin slab parallel to the haem at a distance of 3.2±0.3 Å from the haem plane. The allowed region in the direction perpendicular to the haem is determined by the haem on one side and mainly by residue Leu 29 on the other side (Fig. 1). The average distance from the haem plane seen in this study agrees with the value of Schlichting *et al.*[10] who found 3.1 Å; Teng *et al.*[11] observe tilted CO molecules so one atom is 2.8 Å from the plane and the other is at 3.0 Å. The study of Hartmann *et al.*[12] observed both positions.

The CO molecule has considerably more freedom in the plane parallel to the haem (see Fig. 2). It occupies an L-shaped area about 2.5–3 Å in length mainly over the NC pyrrole haem ring. There are two high probability regions marked 1 and 2 on Fig. 2, which correspond approximately to the centroids of the positions observed by Schlichting *et al.*[10] and by Teng *et al.*[11]. The projections of the CO coordinates from the X-ray structures are shown in Fig. 2; the length of the CO molecule projection from the Teng *et al.*[11] structure is slightly less than that of Schlichting *et al.*[10] because the CO in the former is tilted somewhat relative to the haem. The CO molecule can move closer to the iron atom along a direction half way between the NC and NB haem rings; the NB ring is situated below the *x*-axis in Fig. 2. The pocket-forming residues Leu 32, Phe 33, Phe 43, His 64, Val 68, Ile 107 are the main determinants of the CO distribution in the plane parallel to the haem (Fig. 1). In position 1 (closer to the haem iron) the CO is in van der Waals contact with His 64, Val 68, Leu 29, Phe 43 and the haem; in position 2 (further from the iron) the CO is in contact with Phe 43, Ile 107, Leu 29 and the haem. The importance of these residues in forming the haem pocket and mediating ligand rebinding has been discussed in earlier work[5,7–9]. The fact that the two positions observed by Schlichting *et al.*[10] and Teng *et al.*[11] for the dissociated ligand have high probability in the simulations suggests that they have observed two different CO binding sites in the haem pocket, while Hartmann *et al.*[12] observed both sites. Further, it indicates that the low temperature and room temperature data can be compared, in accord with the interpretation of spectroscopic measurements[4,13–17]. One possible explanation of the difference in position found in the three experiments is that they were done at different temperatures. It has been observed that in the temperature range between 10 and 20 K there are large variations in the relative population of photodissociated states with only small changes in temperature[17]. Other differences in the experimental protocols used to obtain the dissociated states[10–12] could contribute to the shift in the populations between the two major sites.

Fig. 3 shows the distribution of the angle of the CO molecule relative to the haem normal *versus* the distance to the centre of CO molecule from a line perpendicular to the haem, with its origin at the iron atom. There are two preferred angular orientations of the CO molecule with respect to the haem normal. Peak 2, which is 1.9–2.3 Å from the haem normal, corresponds to a CO molecule oriented at an angle of about 90°–100°. This position is similar to that found by Schlichting *et al.*[10]. In their structure, the angle is close to 90° and the distance of the CO geometric centre from the haem normal is about 1.9 Å. The other peak, marked 1, corresponds to a CO molecule oriented at an angle of about 130° to the haem normal at a distance of 1.1–1.5 Å. This peak is similar to the one found by Teng *et al.*[11]; they reported a 114° tilt (or 180°–114°=66° depending on CO orientation, see Fig. 3) and a separation of about 1.2 Å from the haem normal.

When the CO is far from the iron (as in position 2 on Figs 2 and 3), it rotates relatively freely in the plane parallel to the haem. The tilt of the CO with respect to the haem normal increases as it approaches a position over the iron. The repulsive

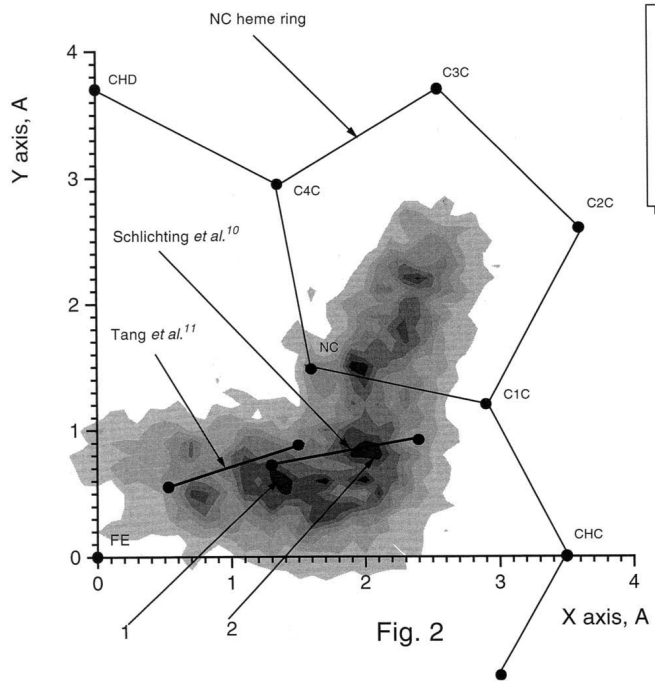

Fig. 2 Probability distribution of CO molecule in the *XY* (haem) plane. Geometric centre of the molecule was used to identify CO position. The difference in grey scale of various (*x*,*y*) positions in the picture represents the relative probability of CO molecule having this position during all dissociation trajectories. The graph was not normalized and the colour depth represents actual number of 'events' (number of CO molecule observations at that position). The projection of the haem NC pyrrole ring and the CO positions from low temperature structures of Schlichting *et al.*[10] and Teng *et al.*[11] are shown. The haem iron projection is at (0,0).

steric interaction with His 64, Leu 29 and the haem (Fig. 1) are primarily responsible for the tilting of the ligand. After dissociation, because of the favourable interactions with the free CO ligand, the distal histidine moves slightly into the pocket. The difference in the average value of χ^1 dihedral angle for His 64 during dissociated dynamics and heat for the CO bound structure[18] is about 10°. When the ligand is close to the iron (position 1 on Figs 2 and 3) it makes an angle of about 130° with respect to the haem plane, which corresponds to an orientation with the carbon atom pointing away from the iron. The orientational preference arises from a combination of nonbonded electrostatic and van der Waals interactions of the CO with the haem and the distal histidine; electrostatic interactions of CO with the proximal histidine also contribute to the stability of CO orientation with the oxygen atom close to the iron. Thus, on photodissociation the CO may rotate so that the O is closer to the haem iron. This could explain why the CO molecule at only 1 Å from its bound position, as found by Teng *et al.*[10] and Hartmann *et al.*[12], rebinds slowly enough to be observed at low temperature. Teng *et al.*[11] suggested this as a possibility, although they were unable to determine which atom (C or O) is closer to the iron. Since the same limitation applies to EXAFS[19,20] and to infrared studies[13,14], the molecular dynamics simulations provide information not available directly from experiment.

The CO orientation with the oxygen atom close to the haem iron could explain the anomalous dependence of the rate of molecular tunnelling on the CO isotopic mass found by Alben *et al.*[21]. In that study it was observed that $^{13}C^{16}O$ rebinds more slowly at 20 K than the slightly heavier $^{12}C^{18}O$, in disagreement with a simple tunnelling model for the rebinding, in which only the total mass of the molecule is considered in determining the rate. Alben *et al.*[21] suggested that the observed isotope dependence could be explained if a rotational motion around an axis perpendicular to the CO vector were involved. If the CO molecule is preferentially oriented with the oxygen atom toward the iron, rebinding would require a rotation of the ligand. The unfavourable orientation also could contribute to slowing the CO geminate rebinding[14,22] relative to physiological ligand O_2.

Analysis of electron density

To obtain a better understanding of the significance of the X-ray results for a mobile ligand like dissociated CO in the haem pocket, we have generated crystallographic X-ray reflections from the

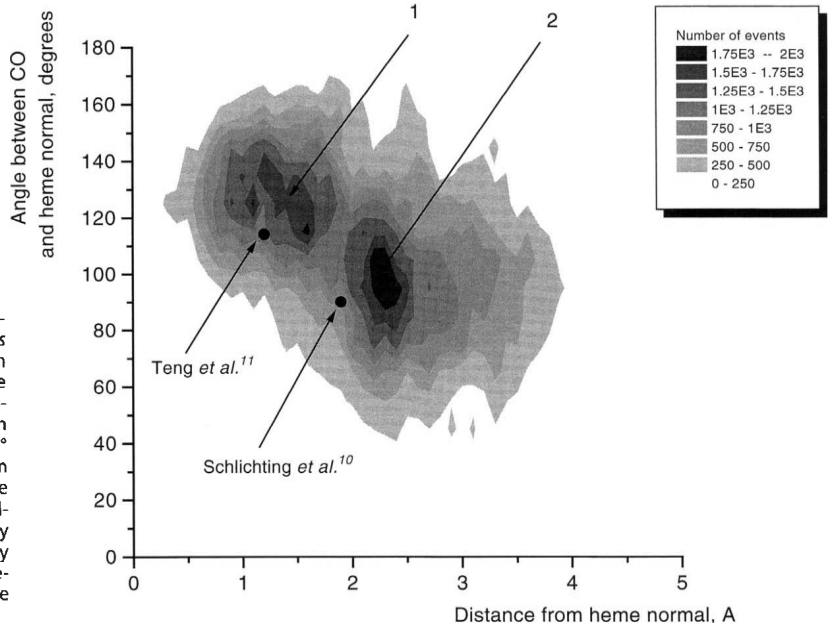

Fig. 3 Probability distribution of the angle CO molecule makes with respect to the haem normal *versus* distance from the CO geometric centre to the haem normal, with it origin at the haem iron atom. The angle is defined as the angle between vector pointing from carbon to the oxygen atom and the haem normal. By this definition if the angle is between 0° and 90° the carbon atom of CO is closer to the haem iron, and if the angle is between 90° and 180° the oxygen atom is closer to the iron. Points corresponding to Schlichting *et al.*[10] and Teng *et al.*[11] X-ray structures are shown on the figure. The probability density maxima marked 1 and 2 on the picture correspond directly to maxima 1 and 2 in Fig. 2. Grey scale in the figure has the same meaning as in the Fig. 2.

molecular dynamic trajectories and refined the myoglobin structure against the calculated reflections by standard methods. The undissociated X-ray structure[22] was used as the initial model (see Methods). The accuracy of the refinement can be tested by comparing the results with those calculated directly from the MD simulation used to generate the X-ray reflections. As has been pointed out by Kuriyan *et al.*[23] this self-consistent approach is free from experimental errors and avoids problems due to errors in the simulation results.

A superposition of the experimental structures of Schlichting *et al.*[10] and Teng *et al.*[11] with that obtained from the refinement based on the molecular dynamics data (Fig. 4) shows that the three structures are very similar. The overall backbone r.m.s.d. between the Teng *et al.*[11] structure and that obtained from the present refinement is 0.86 Å; that between the Schlichting *et al.*[10] structure and the present refined structure is 0.73 Å., for comparison the backbone r.m.s.d. between Schlichting *et al.*[10] and Teng *et al.*[11] is 0.49 Å. The refined molecular dynamics structure is thus a good model for photolysed myoglobin.

A top view of the haem pocket (Fig. 4*a*), presents a clear picture of the CO positions in the three structures. The position of the CO molecule obtained from the molecular dynamics-based refinement (yellow in Fig. 4), the position found by Teng *et al.*[11] (red) and the position found by Schlichting *et al.*[10] (blue) are spatially close. In each case only a single CO was used in the refinement. The figure confirms the fact, already clear from the distribution plots (Figs 2, 3), that the CO distribution has high probability in the region found by the low temperature X-ray studies.

Fig. 5 shows in red the $(2F_o–F_c)$ electron density map at the 1σ level obtained after the structure refinement based on the reflections calculated from the simulations. The blue contours in the figure correspond to the density map generated only by CO molecules. It is shown at the 1σ level and is calculated directly from the dissociation trajectories without refinement (see Methods). The position of the CO obtained from the refinement (see Fig. 4*b*) is also shown. Comparison of the red and blue contours shows that the density from the refinement substantially underestimates the spatial distribution of the CO in the haem pocket. Similar results are obtained from the $(F_o–F_c)$ omit map. It is not possible to enlarge the refined CO distribution by use of lower contour levels because the maps become too noisy to discern any features.

That crystallographic refinements underestimate the range of positions of mobile protein atoms was noted previously[23,24]. In this case the effect is very pronounced because of the extended distribution of the CO in the haem pocket (Fig. 2). The underestimation of the extent of the CO distribution occurs because the average electron density of the distributed CO is smaller than that for the majority of protein atoms. Thus, the map at a 1σ level includes only part of the region where CO is found; that is, the part with the highest density. The rest of the density generated by CO molecules is non-interpretable because it is below the noise level. The refinement of the experimental X-ray data for

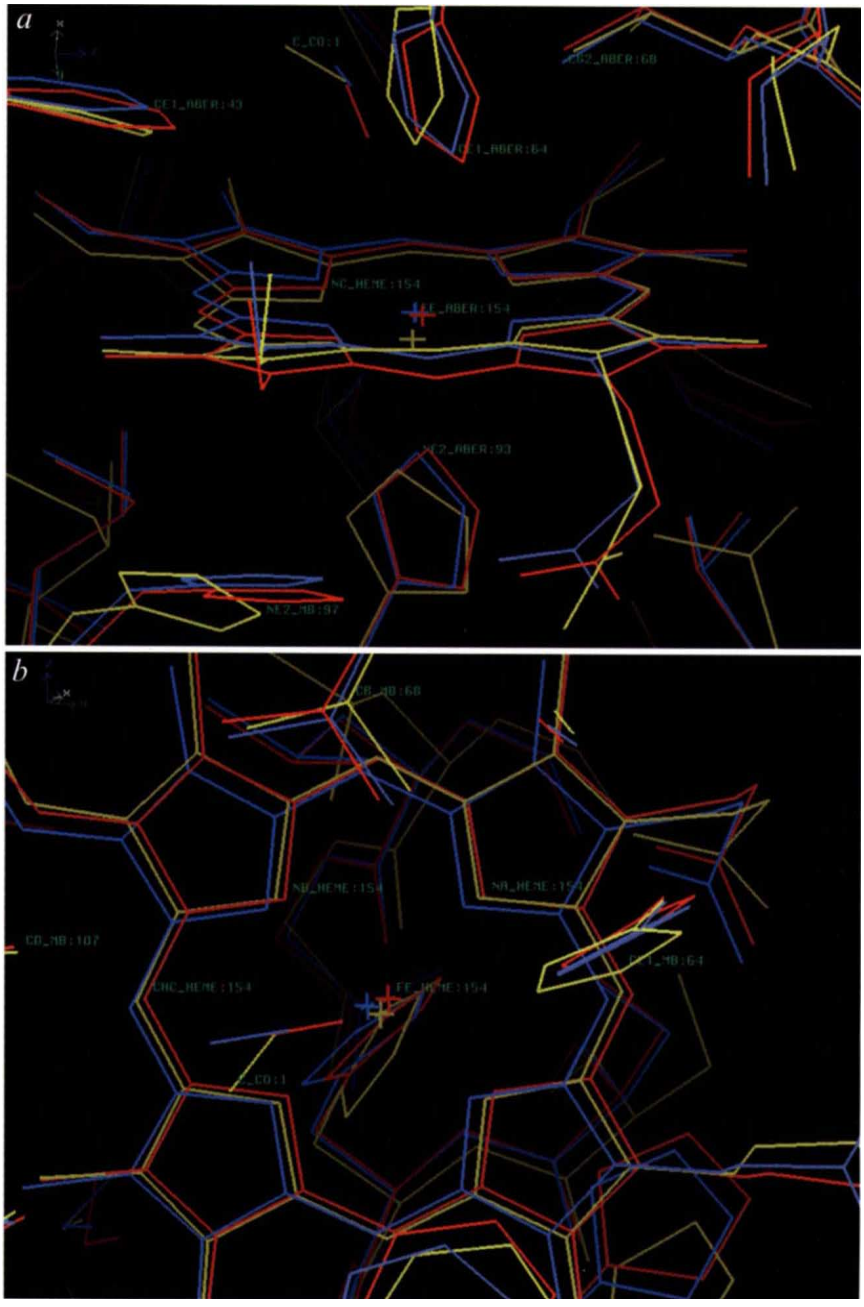

Fig. 4 *a*, Superposition of three myoglobin structures. The structure obtained based on the refinement in this paper is yellow; the structure obtained by Schlichting *et al.*[10] in blue; the structure obtained by Teng *et al.*[11] in red. The structures were superimposed based on the r.m.s. deviation of the haem pocket forming residue: Leu 29, Leu 32, Phe 33, Phe 43, His 64, Val 68, Ile 107 and the haem. The view on the picture is from the side into the haem pocket. *b*, The same superimposed structures as in (*a*). The view is from the distal side from above the haem into the haem pocket.

photodissociated CO[10–12] is likely to have similar problems so that the CO positions reported by Schlichting *et al.*[10] and Teng *et al.*[11] may not fully represent the extended CO distribution function in the pocket.

The molecular dynamic simulations of the CO molecule in the myoglobin haem pocket after photodissociation provide an essential complement to recent low temperature X-ray crystallographic studies[10–12]. The distribution function of CO is broad with significant coupling between the CO position and its orientation relative to the haem. There are two preferred positions in the pocket, one of which is significantly closer to the haem iron than the other. The two observed high probability sites are close to those found in low temperature X-ray structures. The simulations indicate that both sites have at least a short time stability at room temperature, in agreement with femtosecond infrared measurements. In the simulation analysis and the interpretation by Schlichting *et al.*[10] and by Teng *et al.*[11], both positions correspond to unliganded CO in the haem pocket. Hartmann *et al.*[12] have suggested that the closer site observed by Teng *et al.*[11] is bound (or rebound) CO. This seems unlikely because the observed distance of the nearest CO atom from the iron is 2.6 Å, as compared with the expected value of about 1.85 Å. To justify their conclusion, Hartmann *et al.*[12] point out that when the CO position is refined against data for ligated CO, without restraints on the Fe–C bond, the CO moves away from the iron to a position where the Fe–C distance is about 2.1 Å. This results may be due to the fact that the CO ligand is going toward the nearest nonbonded local minimum[25] in the refinement, but is restrained from reaching it by the X-ray data.

The simulation identifies the atom which is closer to the iron in the Teng *et al.*[11] structure as an oxygen. This would be expected to slow the rate of geminate CO rebinding. Such an orientation of the CO molecule could also explain the anomalous isotope effect observed for CO rebinding in the tunnelling regime

In the electron density map generated from the dissociated molecular dynamic trajectories, the distribution of CO molecules in the haem pocket is such that it should be possible to observe localized density for CO at room temperature if the time-resolution of the X-ray experiment is greater than the characteristic time of CO in the pocket after dissociation and before diffusion into the solvent. Since this time is estimated from spectroscopic studies to be more than a hundred nanoseconds[13], time resolved X-ray studies of the system should be possible[26,27] (see note added in proof).

The differences between the distribution of CO from the refinement of X-ray data generated by the simulation and the actual calculated distribution from the same simulation suggest certain difficulties in the interpretation of time resolved X-ray spectra. The refined density was shown to significantly underestimate the actual distribution. This effect is expected to occur for any mobile group for which significant time and spatial averaging occur during the experiment. Such phenomena are intrinsic to time resolved X-ray crystallography, but may also have to be considered in the interpretation of the electron density of highly mobile atoms and molecules (such as some water molecules on the protein surface[28]) obtained by data collection on the usual time scales.

Methods

Potential function and molecular dynamic parameters. Standard molecular dynamics methodology was employed and the program CHARMM[29] was used for the calculations. The all-hydrogen topology with parameter set 22 was employed. The haem parameters for carboxy and deoxymyoglobin were the same as in Kuczera *et al.*[30] A slightly modified TIP3P model[31] was used to represent water molecules. A switch function was used to truncate the van der Waals interactions over 10–12 Å and a shift function with a 12 Å cutoff was used to truncate the electrostatic interactions[32]; a dielectric constant of unity was used to be consistent with the parameter set. The SHAKE algorithm[33] was employed to constrain hydrogen atoms during the simulation. An integration time step of 1 fs was used. The distal histidine (His 64) was kept neutral to reflect the pH of the low temperature crystal structures. For the CO molecule the quadrupolar model developed by Straub *et al.*[6] was used. This model represents the CO molecule as a system with two van der Waals spheres and three charged sites.

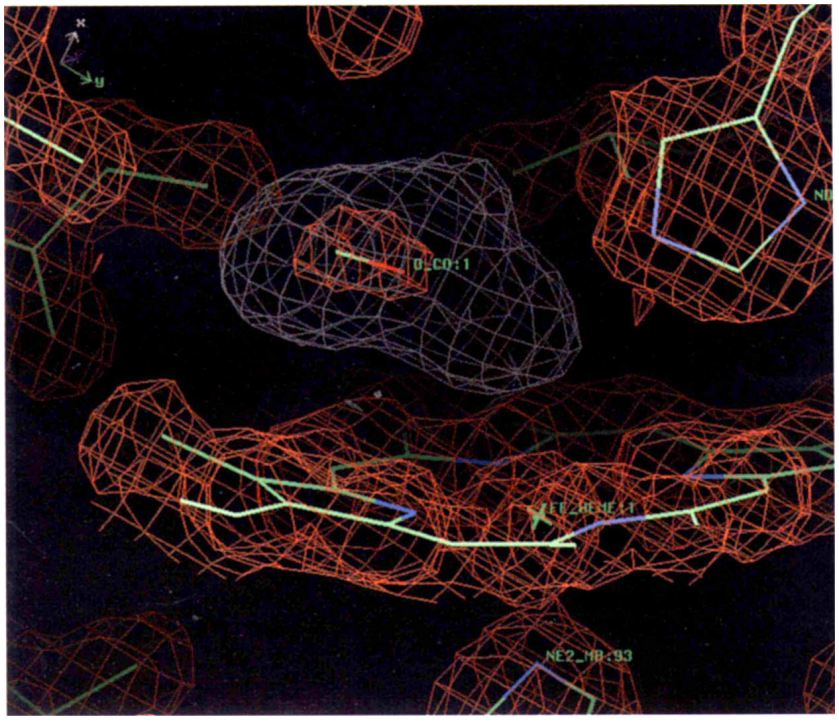

Fig. 5 A close view of the haem pocket. The red electron density represents ($2F_o$–F_c) map obtained by refinement in the present paper. The blue density represents electronic density generated only by unbound CO molecules in the haem pocket. The densities are drawn at their respective 1σ levels.

Simulation system. The crystal structure by Kuriyan *et al.*[18] was used as the starting model for the simulations. Hydrogen atoms were build into the structure with the HBUILD[34] module in CHARMM. A shell of 492 water molecules was used to solvate the system[35]. No crystal waters from the crystal structure of Kuriyan *et al.*[18] were included. After minimization for 400 steps with ABNR method, 5 ps heating and 50 ps equilibration, a molecular dynamic run of 300 ps of MbCO was calculated to generate the initial configurations for the CO dissociation studies. The r.m.s. deviation from X-ray structure during production run stabilized at 0.9 Å for backbone atoms and 1.3 Å for all atoms. The r.m.s. deviation for backbone atoms of pocket forming residues (Leu 29, Leu 32, Phe 33, Phe 43, His 64, Val 68, Ile 107 and the haem stabilized) at 0.7 Å.

Dissociation protocol. To obtain starting structures for CO dissociation, 28 configurations from the undissociated myoglobin simulation were selected; they were separated from each other by 10 ps. Photodissociation was simulated by instantaniously changing the haem parameters to those for unliganded haem and including only nonbonded interactions between the haem and the CO. For each dissociated system, simulations 10 ps in length were performed using the same protocol as that for the undissociated myoglobin system. The final 9 ps of each dissociation trajectory were used in generating the results since it was observed that the CO distributions were independent of time if the first ps was omitted.

X-ray reflection and electron density generating protocol. Average crystallographic reflections were obtained from the trajectory by the same procedure as used by Kuriyan *et al.*[23] in their analysis of myoglobin X-ray refinement. For the calculation of the reflections, the protein crystal was assumed to be monoclinic and have the $P2_1$ space group. The unit cell parameters were taken from the myoglobin structure of Kuriyan *et al.*[18]; they are: a=64.1 Å; b=30.84 Å; c=34.69 Å; α=90°; β=105.84°; γ=90°; The unit cell parameters are very close to those found by Teng *et al.*[11]. The crystallographic reflections were generated in a 10 Å–1.5 Å resolution range. A total of 21149 unique reflections are available in this resolution range for assumed crystal form of myoglobin. 180 coordinate sets with a separation of 50 fs along the trajectories were taken from each of the 28 dissociation runs. All unique reflections were generated from each set using the program X-PLOR[36]. The intensities were averaged over all coordinate sets from the 28 trajectories. No explicit experimental noise was introduced during generation of the reflections. Water molecules were excluded in generating the reflections to decrease noise and simplify analysis of the density.

Structure refinement. The myoglobin structure was refined against the calculated intensities obtained from the dissociation trajectories with the Kuriyan *et al.*[18] structure as the initial model for obtaining phase information. The refinement was done with program X-PLOR[36]. The parameter set (CHARMM 22) used in the molecular dynamic simulations was used in the X-PLOR refinements. All 21149 unique reflections were used in refinement, thus, the completeness of the reflection data was 100%. No water molecules were added in the refinement as they were excluded in generating the reflections and thus did not appear in the electron density map.

The initial R-factor for the structure was 36.7% for the data from 10–1.5 Å resolution. First, several cycles of positional refinement were performed. Then manual rebuilding and corrections were done on the basis of inspection of the $(F_0–F_c)$ and $(2F_0–F_c)$ electron density map; a few side chains on the protein surface far from the binding site had to be reoriented. The $(2F_0–F_c)$ and $(F_0–F_c)$ electron maps of the haem pocket were inspected and density was found in the place where the CO was likely to be in the molecular dynamic simulations. The CO molecule was modeled into the density with the oxygen atom closer to the haem iron (the orientation used by Schlichting *et al.*[10]) and positional refinement was continued. The R-factor at the end of the positional refinement decreased to 24%. Then group and individual B-factor refinement was done. Also the occupancy for CO molecule was refined. The final R-factor for the structure was 22.5%. The occupancy for CO molecule was as follows: for the C atom, 0.54, for the O atom, 0.46. For comparison, in the low temperature structure of Teng *et al.*[11] the occupancy was: for the C atom 0.62, for the O atom 0.52; in the structure of Schlichting *et al.*[10] the occupancy was: for the C atom 1.0, for the O atom 0.88.

Generation of electron density due to the CO molecules. To compare with the electron density map obtained by the X-ray refinement of the simulation data, the density generated by an ensemble of CO molecules from the dissociation trajectories was calculated. The density was obtained by taking CO positions from each trajectory frame (180 frames per trajectory) of all 28 dissociation trajectories and generating the density from every CO position on a three-dimensional grid using X-PLOR[36]. Individual densities were than added and averaged at each grid point.

All the calculations were done on Hewlett-Packard 735/125 workstations. Figs 2 and 3 were generated using MicroCal Origin 3.0 (MicroCal Software, Inc.). Figs 4 and 5 were generated using Quanta 4.1 (Molecular Simulations, Inc.).

The coordinated of the refinement based on the molecuar dynamics simulation can be obtained from *marci@tammy.harvard.edu*.

Acknowledgements

We thank K. Moffat and J. Berendzen for providing us with coordinates of dissociated MbCO intermediates. We also thank P. Anfinrud and D. Ringe for helpful discussions. We are grateful to D. Peisach for help in generation of the figures. This work is supported in part by grants from NIH to MK and GP.

Note added in proof: While this manuscript was under review, a paper was published[37] that described structural data obtained for photodissociated MbCO with a time resolution of 4–9 ns. In agreement with our calulations, the density of the photodissociated CO was observed and it was in the region predicted by the present report. Also, the displacement of the distal histidine is in the direction found in the simulations and differs from that observed in the low temperature study of Schlichting et al.[10].

Received 17 September 1996; accepted 3 January 1997.

1. Antonini, E. & Brunori, M. Haemoglobin and myoglobin in their reactions with ligands. (North-Holland, London, 1971).
2. Springer, B. A., Sligar, S. G., Olson, J. S. & Phillips, Jr. G. N. Mechanisms of ligand recognition in myoglobin. *J. Chem. Rev.* **94**, 699–714 (1994).
3. Collman, J. P., Brauman, J. I., Halbert, T. R. & Suslick, K. S. Nature of O_2 and CO binding to metalloporphyrins and haem proteins. *Proc. Natl. Acad. Sci. USA* **73**, 3333–3337 (1976).
4. Ansari, A. *et al.* Rebinding and relaxation in the myoglobin pocket. *Biophys. Chem.* **26**, 337–355 (1987).
5. Elber, R. & Karplus, M. Enhanced sampling in molecular dynamics: Use of the time-dependent Hartree approximation for a simulation of carbon monoxide diffusion through myoglobin *J. Am. Chem. Soc.* **112**, 9161–9175 (1990).
6. Straub, J. & Karplus, M. Molecular dynamics study of the photodissociation of carbon monoxide from myoglobin: ligand dynamics in the first 10 ps. *Chem. Phys.* **158**, 221–248 (1991).
7. Gibson, Q. E., Regan, R., Elber, R., Olson, J. S. & Carver, T. E. Distal pocket residues affect picosecond ligand recombination in myoglobin. *J. Biol. Chem.***267**, 22022–22034 (1992).
8. Carlson, M. L. *et al.* Nitric oxide recombination to double mutants of myoglobin:role of ligand diffusion in a fluctuating haem pocket. *Biochemistry* **33**, 10597–10606 (1994).
9. Li, H., Elber, R. & Straub, J. E. Molecular dynamics simulation of NO recombination to myoglobin mutants. *J. Biol. Chem.* **268**, 17908–17916 (1993).
10. Schlichting, I., Berendzen, J., Phillips, Jr. G. N. & Sweet, R. M. Crystal structure of photolyzed carbonmonoxymyoglobin. *Nature* **371**, 808–812 (1994).
11. Teng, T.-Y., _rajer, V. & Moffat, K. Photolysis-induced structural changes in single crystals of carbonmonoxymyoglobin at 40K. *Nature Struct. Biol.* **1**, 701–705 (1994).
12. Hartmann, H. *et al.* X-ray structure determination of a metastable state of carbonmonoxy myoglobin after photodissociation. *Proc. Natl. Acad. Sci. USA* **93**, 7013–7016 (1996).
13. Lim, M., Jackson, T.A. & Anfinrud, P.A. Binding of CO to myoglobin from a haem pocket docking site to form nearly linear Fe-C-O. *Science* **269**, 962–966 (1995).
14. Lim, M., Jackson, T.A. & Anfinrud, P. A. Mid-infrared vibrational spectrum of CO after photodissociation from haem: Evidence for a ligand docking site in the haem pocket of haemoglobin and myoglobin. *J. Chem. Phys.* **102**, 4355–4366 (1995).
15. Petrich, J.W., Poyart, C. & Martin, J.L. Photophysics and reactivity of haem proteins: A femtosecond absorption study of haemoglobin, myoglobin, and protohaem. *Biochem.* **27**, 4049–4060 (1988).
16. Anfinrud, P.A., Han, C. & Hochstrasser, R.M. Direct observation of ligand dynamics in haemoglobin by subpicosecond infrared spectroscopy. *Proc. Natl. Acad. Sci.USA* **86**, 8387–8391 (1989).
17. Alben, J. O. *et al.* Infrared spectroscopy of photodissociated carboxymyoglobin at low temperatures. *Proc. Natl. Acad. Sci. USA* **79**, 3744–3748 (1982).
18. Kuriyan, J., Wilz, S., Karplus, M. & Petsko, G.A. X-ray structure and refinement of carbon-monoxy myoglobin at 1.5 Å resolution. *J. Mol. Biol.* **192**, 133–154 (1986).
19. Teng, T.-Y., Huang, H. W. & Olah, G. A. 5K extended X-ray absorption fine structure and 40 K 10-s resolved extended X-ray absorption fine structurestudies of photolyzed carboxymyoglobin. *Biochemistry* **26**, 8066–8072 (1987).
20. Powers, L. *et al.* Kinetic, structural, and spectroscopic identification of geminatestates of myoglobin: A ligand binding site on the reaction pathway. *Biochemistry* **26**,4785–4796 (1987).
21. Alben, J.O. *et al.* Isotope effect in molecular tunneling. *Phys. Rev. Letts.* **44**, 1157–1160 (1980).
22. Jongeward, K.A. *et al.* Picosecond and nanosecond geminate recombination of

myoglobin with CO, O^2, NO, and Isocyamides. *J. Am. Chem. Soc.* **110**, 380–387 (1988).
23. Kuriyan, J., Petsko, G.A., Levy, R.M. & Karplus, M. Effect of anisotropy and anharmonicity on protein crystallographic refinement. *J. Mol. Biol.* **190**, 227–254 (1986).
24. Ichiye, T. & Karplus, M. Anisotropy and anharmonicity of atomic fluctuations inproteins: implications for X-ray analysis. *Biochemistry* **27**, 3487-3497 (1988).
25. Sassaroli, M. & Rousseau, D.L. Simulation of carboxymyoglobin photodissociation. *J. biol. Chem.* **261**, 16292–16294 (1986).
26. Hajdu, J. & Andersson I. Fast Crystallography and time-resolved structures. *Annu. Rev. Biopys. Biomol. Struct.* **22**, 467–497 (1993).
27. Bourgeois, D. *et al.* Single pulse Laue images from macromolecular crystals recorded at ESRF. *SPIE* **2521**, 178–181 (1996).
28. Levitt, M. & Park, B.H. Water: now you see it, now you do not. *Structure* **1**, 223–226 (1993).
29. Brooks, B.R. *et al.* CHARMM: A program for macromolecular energy, minimization, and dynamic calculations. *J. Comp. Chem.* **4**, 187–217 (1983).
30. Petrich, J.W. *et al.*Ligand binding and protein relaxation in haem proteins: A room temperature analysis of NO geminate recombination. *Biochemistry* **30**, 3975–3987 (1991).
31. Jorgensen, W.L., Chandrasekhar, J., Madura, J.D., Impey, R.W. & Klein, M.L. Comparison of simple potential functions for simulating liquid water. *J Chem. Phys.* **79**, 926-935 (1983).
32. Loncharich , R.J. & Brooks, B.R. The effects of truncating long-range forces on protein dynamics. *Proteins* **6**, 32–45 (1989).
33. Van Gunsteren, W.F. & Berendsen, H.J.C. Algorithms for molecular dynamics and constraint dynamics. *Mol. Phys.* **34**, 1311–1327 (1977).
34. Brünger, A.T. & Karplus, M. Polar hydrogen in proteins:empirical energyplacement and neutron diffraction comparison. *Proteins* **4**, 148–156 (1988).
35. Steinbach, P. J. & Brooks, B. R. Protein hydration elucidated by molecular dynamics simulation. *Proc. Natl. Acad. Sci. USA* **90**, 9135–9139 (1993).
36. Brünger, A.T., Kuriyan, J. & Karplus, M. Crystallograpic R factor refinement by molecular dynamics. *Science* **235**, 458–460 (1987)
37. Srajer, V. *et al.* Monoxide of myoglobin: nanosecond time-resolved crystallography. *Science* **274**, 1726–1729 (1996).